NUCLEAR INSTRUMENTS AND METHODS 145 (1977) 295-310 ; © NORTH-HOLLAND PUBLISHING CO.

γ-RAY MULTIPLICITIES FROM NUCLEAR REACTIONS: THEORY, INSTRUMENTATION AND ANALYSIS

L. WESTERBERG, D. G. SARANTITES, R. LOVETT, J. T. HOOD

Department of Chemistry, Washington University, St. Louis, Missouri 63130, U.S.A.

J. H. BARKER

Department of Physics, St. Louis University, St. Louis, Missouri 63103, U.S.A.

C. M. CURRIE and N. MULLANI

Radiation Sciences, Washington University, St. Louis, Missouri 63130, U.S.A.

Received 23 March 1977

Expressions for interpreting γ-ray multiplicity measurements with a Ge(Li) and N NaI detectors are derived. A scattering chamber designed to allow measurements of multiple coincidences between a Ge(Li) detector and/or particle detectors and up to 12 NaI detectors is described. A special multiplicity recording unit has been constructed. It employs the strobed overlap coincidence technique and it is suitable for routing a multichannel analyzer or for interfacing to a computer. Details of the analysis procedure are discussed. The application of a computer code to multiplicity calculations is described.

1. Introduction

There are several classes of nuclear reactions in which knowledge of the number of emitted γ-rays is of importance. In heavy-ion induced reactions, for example, knowledge of the number of γ-rays from the emitted heavy-ion transfer products as well as their energy spectrum is important in understanding the de-excitation processes involved. In heavy-ion induced fusion reactions in the regions of deformed nuclei, knowledge of the first few moments of the distribution in the number of γ-rays can be used to infer the angular momentum distributions in the product nuclei or even in the compound system. Finally in light-ion induced fusion reactions describable by the compound statistical or by the hybrid model for nuclear reactions, measurements of the multiplicity of the γ-rays can help in understanding the mechanisms involved.

The simple fact that the coincidence rate in γ–γ coincidence experiments depends upon the number of γ-rays in cascade has only recently been used to deduce the cascade lengths. Multiplicity experiments that employed Ge(Li) and NaI detectors were reported by Tjøm et al.[1]) and Der Mateosian et al.[2]). The former was a two detector experiment that involved a Ge(Li) detector for gating and a single NaI detector as a coincidence counter. Hagemann et al.[3]) later employed a Ge(Li) and four NaI detectors. That arrangement allowed them to deduce not only the average multiplicity but also higher moments of the distribution as well.

In this paper we present in some detail the theory, instrumentation and method of analysis of experiments[4–6]) employing as a strobing device a Ge(Li), a Ge(Li) coincident with several Si or time-of-flight neutron detectors, or a heavy-ion $\Delta E \times E$ detector telescope and a set of eight or nine NaI detectors. The theoretical expressions used to analyze the multiplicity measurements are derived. Two versatile multi-detector scattering chambers and their associated instrumentation are described. Finally, the computational procedure used in the analysis and the necessary corrections to the data are discussed.

2. Theory

In the following, the expressions necessary for the analysis of a multiplicity experiment employing a gating Ge(Li) detector and N NaI counters will be derived.

* Work supported by the U.S. Energy Research and Development Administration.

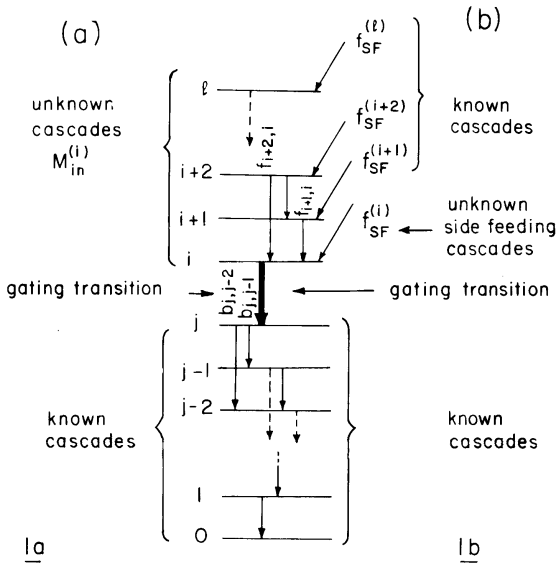

Fig. 1. (a) Decay scheme for simple analysis of multiplicity data, where the cascade entering the level i of the gating transition is taken as the unknown. (b) Decay scheme employed in analyses for the calculation of the side feeding multiplicity entering the ith level. All other transitions and side feedings are considered known.

2.1. Experimentally observed quantities

For simplicity we shall discuss first the case of a cascade of $M_{in}^{(i)}$ γ-rays entering the highest ith state of the ground state band of a typical nucleus (see fig. 1a). More complex situations for levels with side feeding and incoming branched decays (fig. 1b) can also be analyzed and they will be discussed later. Let us label α the γ-ray from the ith to the jth level. This is detected in the Ge(Li) detector [ignoring for the time being summing effects in the Ge(Li)] with a singles rate $Q_s^{(\alpha)}$ given by

$$Q_s^{(\alpha)} = \sigma_i \Omega_{Ge}^{(\alpha)}, \tag{1}$$

where σ_i is the cross section leading to the ith state and $\Omega_{Ge}^{(\alpha)}$ is the efficiency of the Ge(Li) detector, including solid angle, for the full energy peak. The detection of this γ-ray provides the "gate event" and coincidences out of the N idential NaI detectors are examined. The counting rate for a p-fold coincidence from all possible combinations of p detectors that fire is

$$Q_{c,p}^{(\alpha)} = \sigma_i \Omega_{Ge}^{(\alpha)} P_{Np}^{(\alpha)}, \tag{2}$$

where $P_{Np}^{(\alpha)}$ is the overall probability that out of N detectors p of them fire. The quantity $P_{Np}^{(\alpha)}$ of course must account for the probability that any NaI detector recorded one or more photons and for the fact that for each cascade there is a definite angular correlation function. Ignoring, for the moment, the angular correlation effects we note that the probabilities $P_{Np}^{(\alpha)}$ can be obtained from experiments as $Q_{c,p}^{(\alpha)}/Q_s^{(\alpha)}$ or as the ratios

$$P_{Np}^{(\alpha)} = \sum_{\omega} C_{p\omega}^{(\alpha)} \Big/ \sum_{p=0}^{N} \sum_{\omega} C_{p\omega}^{(\alpha)}, \tag{3}$$

where $C_{p\omega}^{(\alpha)}$ are the peak areas corresponding to a particular set of detectors, ω, that registered p-fold coincidences.

2.2. Statistical considerations

It now remains to relate the experimentally observed quantities $P_{Np}^{(\alpha)}$ to the desired moments of the multiplicity distribution.

It will be assumed that there is no spatial correlation among the outgoing γ-rays. Thus the probability that each detector records a particular γ-ray is the same for each detector. It will further be assumed that the known sequence below the triggering γ-ray will have known detection efficiencies, Ω_β, ($\beta = 1,2,...$) which are the same for each of the N detectors. Of course the unknown sequence of $M_{in}^{(i)}$ γ-rays will be characterized less precisely. It will be assumed that each γ-ray will be detected with an average detection probability $\bar{\Omega}$.

A straightforward description of a single event would be to report the numbers $n_1,\ldots,n_N$, where n_j is the number of γ-rays triggering the jth detector. Let the probability of this outcome be $P_{n_1,n_2,\ldots,n_N}$, which in fact is not an experimental quantity. A *generating function* $G(t_1,t_2,\ldots,t_N)$ of the counting variables $t_1,\ldots,t_N$ for the $P_{n_1,n_2,\ldots,n_N}$ may be defined by

$$G(t_1,\ldots,t_N)=\sum_{n_1\ldots n_N} P_{n_1,\ldots,n_N}\, t_1^{n_1}\ldots t_N^{n_N}. \tag{4}$$

The numbers $P_{n_1,\ldots,n_N}$ may be deduced from a knowledge of $G(t_1,t_2,\ldots,t_N)$.

If the γ-rays are divided into two statistically independent groups, labelled ζ and ξ with probabilities $P^{(\zeta)}_{l_1,\ldots,l_N}$ and $P^{(\xi)}_{m_1,\ldots,m_N}$, then counting *both* groups with non-distinguishing detectors leads to

$$P_{n_1,\ldots,n_N}=\sum_{\substack{l_1\ldots l_N\\ m_1\ldots m_N}} P^{(\zeta)}_{l_1,\ldots,l_N}\, P^{(\xi)}_{m_1,\ldots,m_N}\,\delta^{n_1}_{l_1+m_N}\ldots\delta^{n_N}_{l_N+m_N}, \tag{5}$$

and

$$G(t_1,\ldots,t_N)=\sum_{n_1\ldots n_N} t_1^{n_1}\ldots t_N^{n_N}\sum_{\substack{l_1\ldots l_N\\ m_1\ldots m_N}} P^{(\zeta)}_{l_1,\ldots,l_N}\, P^{(\xi)}_{m_1,\ldots,m_N}\,\delta^{n_1}_{l_1+m_1}\ldots\delta^{n_N}_{l_N+m_N} \tag{6}$$

$$=\sum_{\substack{l_1\ldots l_N\\ m_1\ldots m_N}} P^{(\zeta)}_{l_1,\ldots,l_N}\, P^{(\xi)}_{m_1,\ldots,m_N}\, t_1^{l_1+m_1}\ldots t_N^{l_N+m_N}$$

$$=\sum_{l_1\ldots l_N} P^{(\zeta)}_{l_1,\ldots,l_N}\, t_1^{l_1}\ldots t_N^{l_N}\cdot\sum_{m_1\ldots m_N} P^{(\xi)}_{m_1,\ldots,m_N}\, t_1^{m_1}\ldots t_N^{m_N}. \tag{7}$$

That is, the generating function is just the product of the generating functions for the two statistically independent subcollections which are being summed.

Since each γ-ray is statistically independent of the remaining γ-rays $G(t_1,\ldots,t_N)$ is just a product of factors, one from each γ-ray. The βth γ-ray triggers some detector with probability Ω_β and no detector with probability $1-N\Omega_\beta$. This leads to a factor $1-N\Omega_\beta+(t_1+t_2+\ldots+t_N)\Omega_\beta$. Thus

$$G(t_1,\ldots,t_N)=[1-(N-t_1-t_2-\ldots-t_N)\,\bar{\Omega}]^{M^{(i)}_{\text{in}}}\prod_\beta[1-(N-t_1-\ldots-t_N)\,\Omega_\beta]. \tag{8}$$

Therefore, the statistics are completely characterized by the function

$$F(t)=[1-(N-t)\,\bar{\Omega}]^{M^{(i)}_{\text{in}}}\prod_\beta[1-(N-t)\,\Omega_\beta], \tag{9}$$

through

$$G(t_1,\ldots,t_N)=F[t_1+t_2+\ldots t_N]. \tag{10}$$

The fact that p of N detectors each recorded *one or more* γ-rays is identical with the fact that the number of detectors which recorded *no* γ-ray is precisely $N-p$.
Thus
$\delta^{N-p}_{\delta^0_n+\ldots+\delta_n}$
is 1 when this occurs and zero otherwise. Averaging this over all sets of $n_1\ldots n_N$, i.e. all outcomes, then gives P_{Np}, the experimentally measured quantity:

$$P_{Np}=\sum_{n_1\ldots n_N} P_{n_1,\ldots,n_N}\,\delta^{N-p}_{\delta^0_{n_1}+\ldots+\delta^0_{n_N}}. \tag{11}$$

If $F(t)=\sum_{n=0}^{\infty} a_n t^n$, then

$$G(t_1,\ldots,t_N)=\sum_{n=0}^{\infty} a_n(t_1+\ldots+t_N)^n=\sum_{n_1\ldots n_N} a_{n_1+\ldots+n_N}\frac{(n_1+\ldots+n_N)!}{\prod_k n_k!}\,t_1^{n_1}\ldots t_N^{n_N}, \tag{12}$$

so that $P_{n_1,\ldots,n_N} = a_{n_1+\ldots+n_N} \dfrac{(n_1+\ldots+n_N)!}{\prod_k n_k!}$, (13)

and

$$P_{Np} = \sum_{n_1 \ldots n_N} \delta^{N-p}_{\delta^0_{n_1}+\ldots+\delta^0_{n_N}} \frac{(n_1+\ldots+n_N)!}{\prod_k n_k!} a_{n_1+\ldots+n_N} = \sum_{n=0}^{\infty} n!\, a_n \sum_{n_1 \ldots n_N} \delta^{N-p}_{\delta^0_{n_1}+\ldots+\delta^0_{n_N}} \delta^n_{n_1+\ldots+n_N} \frac{1}{\prod_k n_k!}. \tag{14}$$

In the appendix the sum over $n_1 \ldots n_N$ is evaluated as

$$\frac{1}{n!}\binom{N}{p}(-1)^p \sum_{k=0}^{p}\binom{p}{k}(-1)^k k^n,$$

whence

$$P_{Np} = \sum_{n=0}^{\infty} a_n \binom{N}{p}(-1)^p \sum_{k=0}^{p}\binom{p}{k}(-1)^k k^n = (-1)^p\binom{N}{p}\sum_{k=0}^{p}(-1)^k\binom{p}{k}\sum_{n=0}^{\infty} a_n k_n$$

$$= (-1)^p\binom{N}{p}\sum_{k=0}^{p}(-1)^k\binom{p}{k}F(k). \tag{15}$$

This gives a relatively simple prediction for P_{Np} as a sum over the basic structure factor $F(k)$ involving $k = 0, 1, 2, \ldots, p$.

If additional particles – neutrons, for example – are counted by the detectors without discrimination (i.e., they are treated just as γ-rays) then the effect of those additional particles is trivially included by incorporating $1-(N-k)\Omega_n$ factors in $F(k)$ for each such particle. In what follows for integral k the function $F(k)$ will be written as F_k.

Since the Ge(Li) detector actually identifies the triggering γ-ray it is possible to collect data on many different cascades simultaneously. If α labels the triggering γ-ray between levels i and j, *then several collections of data are obtained as sets* $P^{(\alpha)}_{Np}$ with $p = 0, \ldots, N$ for *each* α. Each cascade has its own structure factor $F^{(\alpha)}_k$ and

$$P^{(\alpha)}_{Np} = (-1)^p\binom{N}{p}\sum_{k=0}^{p}(-1)^k\binom{p}{k}F^{(\alpha)}_k, \tag{16}$$

where

$$F^{(\alpha)}_k = [1-(N-k)\,\bar{\Omega}]^{M_{\text{in}}}\, K^{(j)}_{N-k}\, K^{(\text{neut})}_{N-k}, \tag{16a}$$

with

$$K^{(j)}_{N-k} = \sum_{q=0}^{j-1} b_{jq}[1-(N-k)\,\Omega_{jq}]\, K^{(q)}_{N-k} \tag{16b}$$

to be evaluated from the jth state down to the ground state (numbered as 0) using the known NaI γ-ray efficiencies Ω_{jq}, where j and q label the initial and final states. The decay branching ratios b_{jq} for de-excitation of the state j to states q below satisfy

$$\sum_{q=0}^{j-1} b_{jq} = 1.$$

In the recurrence relation (16b) the ground state is numbered 0 and $K^{(0)}_{N-k} = 1$, $K^{(1)}_{N-k} = 1-(N-k)\,\Omega_{10}$, etc. In eq. (16a) $K^{(\text{neut})}_{N-k} = [1-(N-k)\,\Omega_{\text{neut}}]^x$ and it represents the neutron response of the NaI detectors each having an average efficiency Ω_{neut} for neutron detection when the number of emitted neutrons is x. The average efficiency $\bar{\Omega}$ refers to the cascade of $M^{(i)}_{\text{in}}$ γ-rays entering the state i. The probabilities evaluated via eq. (16) correctly account for losses due to coincidence summing in the NaI counters.

In order to extract the moments of the multiplicity distribution one can follow two methods. In the first one, the P-method, the frist term in $F^{(\alpha)}_k$ of eq. (16a) is expanded in powers of $\bar{\Omega}$ to give via eq. (16)

$$\sum_{r=1}^{M_{\mathrm{in}}^{(i)}} \rho_{pr}^{(j)} X_r^{(i)} = P_{Np}^{(\alpha)} - (1+\rho_{p0}^{(j)}), \tag{17}$$

where

$$\rho_{pr}^{(j)} = \binom{N}{p} \frac{1}{r!} \sum_{k=0}^{p} (-1)^{k-p+r} \binom{p}{k} (N-k)^r K_{N-k}^{(j)} K_{N-k}^{(\mathrm{neut})}, \tag{17a}$$

and

$$X_r^{(i)} = \langle M_{\mathrm{in}}^{(i)} (M_{\mathrm{in}}^{(i)}-1) \ldots (M_{\mathrm{in}}^{(i)}-r+1) \rangle (\bar{\Omega}^{(i)})^r. \tag{17b}$$

For a sufficiently high value $p_{\max}$ of the highest fold observed, eqs. (17) can be solved to give a good approximation of $X_r^{(i)}$, with $r = 1, 2, \ldots, p_{\max}$ by setting $M_{\mathrm{in}}^{(i)} = p_{\max}$.

In the second method, the R-method, one can add the experimental $P_{Np}^{(\alpha)}$ values to obtain the experimental $\mathrm{R}_p^{(\alpha)} \equiv P_{pp}^{(\alpha)}$ values via

$$R_p^{(\alpha)} = \frac{1}{\binom{N}{p}} \sum_{k=p}^{N} \binom{k}{p} p_{Nk}^{(\alpha)}. \tag{18}$$

The quantity $R_p^{(\alpha)}$ represents the probability for observing a p-fold coincidence event if only p NaI detectors were present. It is easy to show that

$$R_p^{(\alpha)} = \sum_{k=0}^{p} (-1)^k \binom{p}{k} (1-k\bar{\Omega})^{M_{\mathrm{in}}^{(i)}} K_k^{(j)} K_k^{(\mathrm{neut})}, \tag{19}$$

where

$$K_k^{(j)} = \sum_{q=0}^{j-1} b_{jq}(1-k\Omega_{jq}) K_k^{(q)} \text{ with } K_k^{(0)} = 1, \tag{19a}$$

and

$$K_k^{(\mathrm{neut})} = (1-k\Omega_{\mathrm{neut}})^x. \tag{19b}$$

Expanding eq. (19) in powers of $\bar{\Omega}$ one obtains

$$\sum_{r=1}^{M_{\mathrm{in}}^{(i)}} \lambda_{pr}^{(j)} X_r^{(i)} = R_p^{(\alpha)} - (1+\lambda_{p0}^{(j)}), \tag{20}$$

where

$$\lambda_{pr}^{(j)} = \frac{1}{r!} \sum_{k=1}^{p} (-1)^{k+r} \binom{p}{k} k^r K_k^{(j)} K_k^{(\mathrm{neut})}, \tag{20a}$$

with $X_r^{(i)}$ given by eq. (17b).

Again setting $M_{\mathrm{in}}^{(i)} = p_{\max}$ permits one to solve eqs. (20) for $X_r^{(i)}$, with $r = 1, 2, \ldots, p_{\max}$.

One advantage of the R-method is that it allows one to observe the magnitude of the corrections for coincidence summing effects in each NaI detector from all higher folds $(p+1, p+2, \ldots, p_{\max})$ to each X_p value[3]).

From the $X_r^{(i)}$ values the moments of the multiplicity distribution can be obtained provided the detection efficiencies $\bar{\Omega}$ are known. In general

$$\bar{\Omega} = \Omega_\gamma (1+\alpha_{\mathrm{T}})^{-1} (1-\Omega_0)^{-1}, \tag{21}$$

where Ω_γ is the integral efficiency (full energy and Compton distribution) of one of the N identical NaI counters, α_{T} is the total conversion coefficient and Ω_0 is the overall efficiency of the Ge(Li). The last factor in eq. (21) as far as the multiplicity is concerned corrects[3]) for coincidence summing effects in the Ge(Li) detector.

If angular correlation corrections are to be included, a reasonable approximation can be obtained by ignoring coincidence summing effects in the NaI detector which in our experiments were found to vary between 5% and 12%. In this case it is sufficient to divide the experimental peak areas $[\sum_{\omega} C_{p\omega}^{(\alpha)}]$ of eq. (3) for $p \geq 1$ by $\overline{W}_p^{(\alpha)}$ given by

$$\overline{W}_p^{(\alpha)} = \frac{1}{\binom{N}{p}} \sum_{\omega} W_{p\omega}^{(\alpha)}(\theta_{\mathrm{Ge}}, \theta_1, \ldots, \theta_p), \tag{22}$$

where $W_{p\omega}^{(\alpha)}$ are the p-fold correlation functions corresponding to a given set ω of the p detectors that fired.

From the $X_r^{(i)}$ values the mean values

$\langle M_{\mathrm{in}}^{(i)} \rangle, \langle M_{\mathrm{in}}^{(i)^2} \rangle, \ldots, \langle M_{\mathrm{in}}^{(i)^{p_{\max}}} \rangle$

can be determined from eq. (17b) and these in turn can be used to calculate the higher moments:

$\mu_n = \langle (M_{\mathrm{in}}^{(i)} - \langle M_{\mathrm{in}}^{(i)} \rangle)^n \rangle$

of the distribution of $M_{\mathrm{in}}^{(i)}$ around the average $\langle M_{(i)} \rangle$.

2.3. Multiplicities of side feeding

When unresolved cascades populate observed levels (side feeding) in the reaction products then the moments of the multiplicity distribution for the side feeding into the ith level can be determined from measurement of the $P_{Np}^{(\alpha)}$ probabilities for a given gating γ-ray de-exciting the ith level and populating the jth level below. In what follows the jth level may decay by branching to several levels below and the ith level may be populated by several incoming transitions (see fig. 1b).

In this case eqs. (20) can be modified to read

$$\sum_{r=1}^{p_{\max}} \lambda_{pr}^{(j)} X_r^{(i)} = \frac{1}{f_{\mathrm{SF}}^{(i)}} [R_p^{(\alpha)} - A_p^{(\alpha)}] - (1 + \lambda_{p0}^{(j)}), \tag{23}$$

where $A_p^{(\alpha)}$ accounts for the coincidence probability via known (earlier measured) cascades connecting from above and below to the gating transition and $f_{\mathrm{SF}}^{(i)}$ is the side-feeding fraction entering the ith state.

The detailed evaluation of $A_p^{(\alpha)}$ now depends on the particular decay scheme in each case. For a gating transition α it is given by

$$A_p^{(\alpha)} = \sum_{k=0}^{p} (-1)^k \binom{p}{k} L_k^{(i)} K_k^{(j)} K_k^{(\mathrm{neut})}, \tag{24}$$

where

$$L_k^{(i)} = \sum_{m=i+1}^{l} f_{mi}(1 - k\Omega_{mi}) [L_k^{(m)} + f_{\mathrm{SF}}^{(m)} (1 - k\bar{\Omega}_{\mathrm{SF}}^{(m)}) M_{\mathrm{SF}}^{(m)}], \tag{24a}$$

and $K^{(j)}$ and $K_k^{(\mathrm{neut})}$ are given by eqs. (19a) and (19b), respectively. In eqs. (24a) l is the highest discrete state resolved. The feeding fractions f_{mi} from the states m above into the state i and the side-feeding fraction satisfy

$$f_{\mathrm{SF}}^{(i)} + \sum_{m=i+1}^{l} f_{mi} = 1.$$

In eq. (24a) $M_{\mathrm{SF}}^{(m)}$ and $\bar{\Omega}_{\mathrm{SF}}^{(m)}$ are the average multiplicity and average γ-ray efficiency for the side-feeding entering the state m. In order to determine the moments of the distribution of $M_{\mathrm{SF}}^{(i)}$ the observed levels must be analyzed downward starting from the top level l. It is clear that as one proceeds downward the uncertainties increase progressively since $f_{\mathrm{SF}}^{(i)}$ decrease and the errors from the highest levels propagate downward.

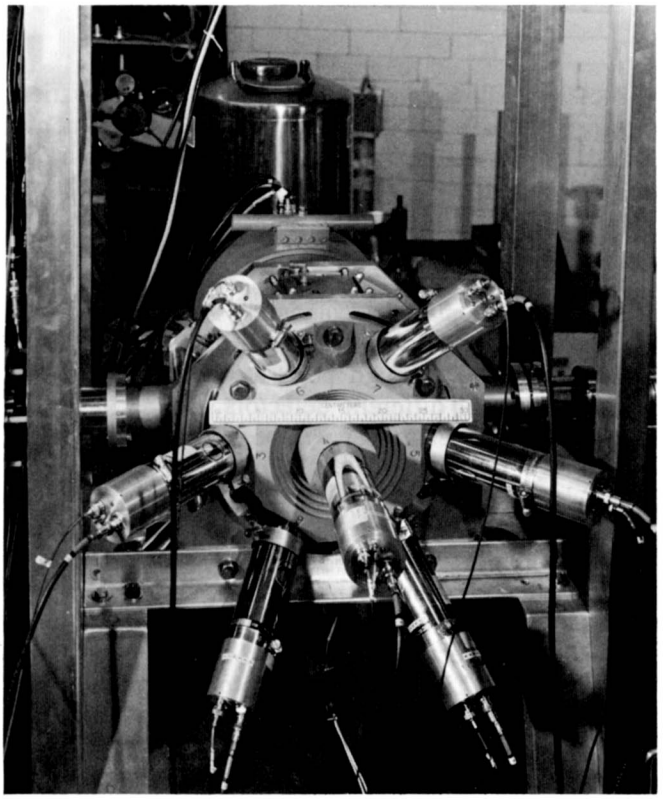

Fig. 2. Lead shield "URCHIN" is seen in the front supporting the NaI detectors. The anti-Compton spectrometer is visible on the other side of the scattering chamber.

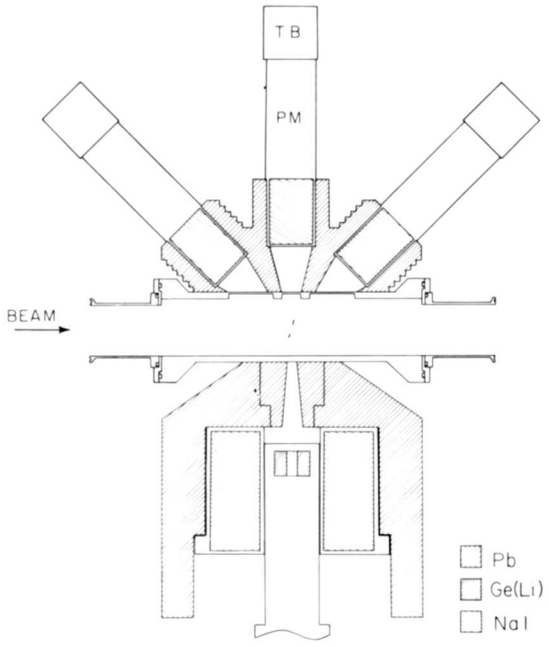

Fig. 3. Cross sectional view of the "URCHIN" and the anti-Compton spectrometer.

3. Instrumentation

3.1. Apparatus

Two scattering chambers were designed and constructed to allow considerable flexibility for a variety of experiments involving γ-ray multiplicity measurements with 9–12 NaI detectors. Each experimental arrangement employs one of the 30.5 cm or 49.5 cm i.d. cylindrical chambers, and a lead shield for seven NaI detectors (URCHIN). The scattering chambers have eight and twelve ports, respectively, on the cylindrical part for inserting detectors, target holder, viewing plate, and beam-line connections.

In all configurations one hemisphere is essentially occupied by the URCHIN lead shield, which supports seven NaI detectors, 5.1 cm diameter by 7.6 cm long with 0.5 mm Cd and 0.1 mm Cu absorbers, at a target to detector distance of 10 cm. Six of the detectors are placed hexagonally at an angle of 45° and the seventh detector is in the middle at 90° to the beam (fig. 2). Up to three additional NaI detectors with separate small lead shields may be placed in either chamber through ports at angles of 90°, 145° or −125° from the beam direction. The positioning of additional different detectors, i.e. a Ge(Li) detector, particle-detector telescopes, neutron detectors, or heavy-ion telescopes will be discussed separately below.

3.1.1. Vertical chamber with an anti-Compton Ge(Li) spectrometer

This arrangement has the scattering chamber mounted in the vertical plane. This allows the anti-Compton spectrometer (19 cm diameter by 14 cm long annular, NaI-crystal) and its shield to be placed at 90° opposite to the URCHIN. In fig. 3 the lead shield surrounding the anti-Compton annulus can be seen opposite to the URCHIN. A typical target to Ge(Li) detector distance is 14 cm. The annulus is shielded from the target by 7.5 cm of lead. In fig. 2 the Ge(Li) and anti-Compton shield are seen on the far side of the 30.5 cm chamber. In this arrangement up to three additional NaI detectors can be placed in the chamber plane through side ports.

The anti-Compton configuration is mainly used in experiments involving only γ-ray detection, since the small solid angle of the Ge(Li) detector makes the coincidence rate with particles very low.

3.1.2. Vertical chamber with a close Ge(Li) detector

Here an additional special lead-shield is used in the place of the anti-Compton assembly. This shield supports a Ge(Li) detector at 90° and two NaI detectors, at 50° and 140° respectively. The target-to-detector distance of the Ge(Li) is 5 cm. Now up to nine NaI detectors are allowed outside the chamber and up to three through the ports making a total of twelve detectors. Two charged particle detectors may also be mounted inside the chamber.

3.1.3. *Horizontal 30.5 cm chamber*

In this configuration the URCHIN can be mounted above or below the chamber. The Ge(Li) detector is inserted through a 90° port. It can be placed at a distance of 7 cm from the target. The lid opposite

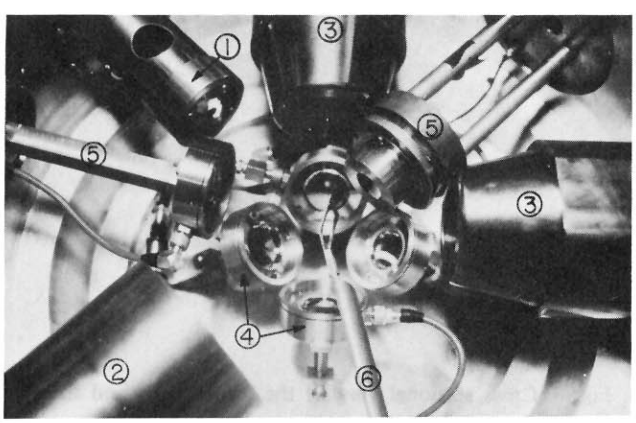

Fig. 4. Photograph of the interior of the scattering chamber. (1) is the beam entrance, (2) shows the Al can housing the Ge(Li) detector, (3) are two Pb shields covering the Al cans of two NaI detectors in the reaction plane, (4) surface barrier detectors below the reaction plane, (5) two additional particle detectors in the plane and (6) the target holder.

to the URCHIN may be opened from below to provide access to the chamber. The lid supports four mounts for particle detectors in the $\pm 55°$ and $\pm 125°$ directions relative to the beam axis outisde the reaction plane opposite to the URCHIN. The detectors mounted inside the chamber can be seen in fig. 4. One can also see two NaI detectors and two Si particle detectors in the reaction plane. In this setup one or two heavy-ion gas-telescopes can be mounted in the chamber plane in the forward quadrants, instead of the light particle detectors[6]). Several neutron detectors can be placed in the reaction plane at distances >50 cm for neutron time-of-flight measurements.

3.1.4. *Horizontal 49.5 cm chamber*

In this arrangement the URCHIN is mounted underneath the cylindrical chamber. The top lid is semispherical to provide room for detectors mounted out of the reaction plane. Two heavy-ion gas-proportional counter $\Delta E \times E$ telescopes can be mounted in the horizontal plane and their angle changed independently while under vacuum. One of the heavy-ion telescopes can also be positioned out of the horizontal plane if so desired. Up to three additional NaI detectors can be inserted through ports. A Ge(Li) detector with a housing of 15 cm of longer can also be inserted via one of the ports (usually at 90°).

3.2. ELECTRONICS

The number of NaI detectors that are in coincidence with a given Ge(Li) event is established in a multiplicity routing-box to be described below. Fast discriminators with adjustable pulse width are used as inputs to the routing-box. These derive their inputs from the NaI anode and Ge(Li) constant fraction discriminator signals. The lower level threshold of the discriminators from the NaI detectors is usually set at ~ 90 keV to avoid triggering on Pb X-rays.

The basic configuration of the multiplicity system is shown in fig. 5. As can be seen, all inputs are on the left side of the diagram and all outputs are on the right. Fig. 6 shows a schematic diagram of the basic electronic circuit of a coincidence latch employed in the multiplicity system.

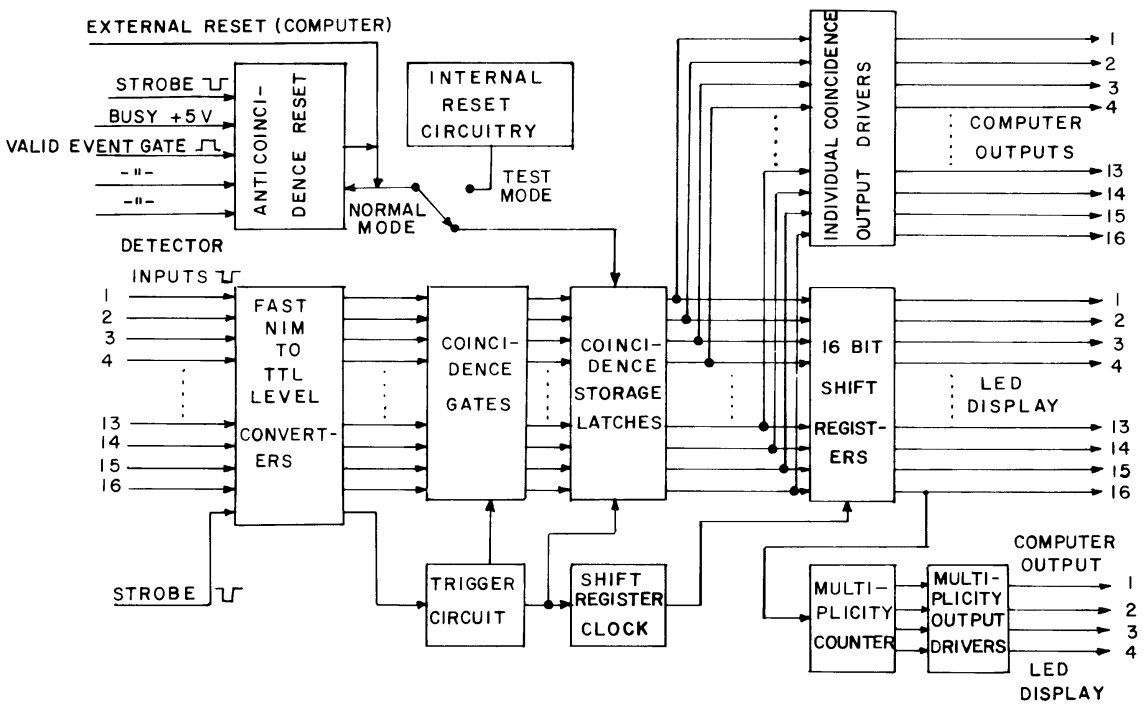

Fig. 5. Functional diagram of the multiplicity routing box.

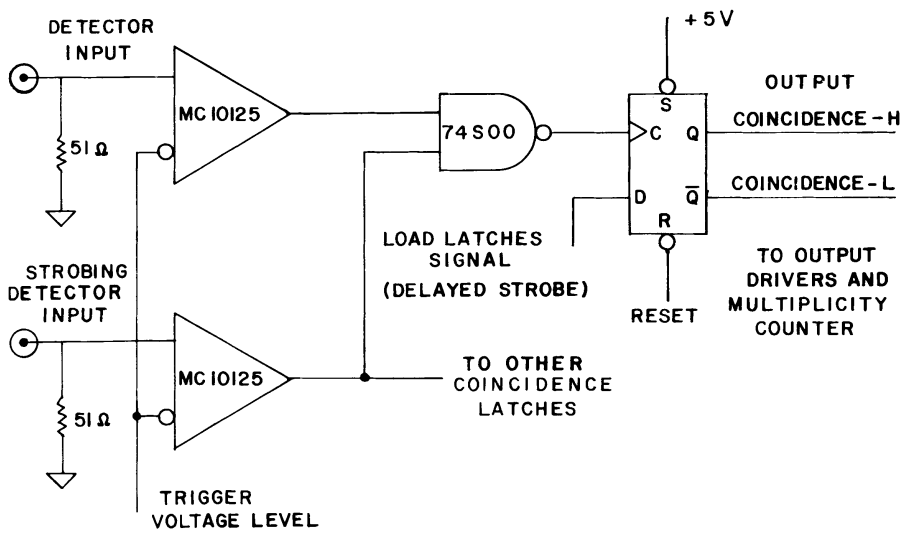

Fig. 6. Schematic diagram of the electronic circuit of the basic coincidence latch used in the multiplicity unit.

The system was constructed to allow up to 16 NaI detectors to be used. A master detector, usually a Ge(Li) or a heavy-ion telescope provides the strobe signal used to establish a coincidence with any number of NaI detectors. Any number of the 16 inputs may be used in a particular application in any combination.

Each of the input signals (normally 0 to -1 V) undergoes a rapid conversion to TTL levels. This allows the major portion of the electronics to be constructed using convenient, inexpensive TTL circuitry.

The outputs of the coincidence gates are then fed into data storage latches to allow sufficient time for the individual detector events to be interrogated and the information sent to a computer. The individual coincidence latches are also loaded into a 16-bit shift register. The register is then shifted 16 times to load the total number of detector coincidences into a four bit counter. This information is also available for computer interrogation.

The two basic modes of operation of the system are the Test mode and the Normal mode. In the Test mode, the multiplicity system is running free and it is reset approximately 2 μs after the strobe event.

In the Normal mode, the computer system controls the collection of data. Initially, the multiplicity system sets the bit latches that hold the information until the computer is ready to accept it. Once the information has been accepted the computer resets the multiplicity system and enables it to collect a new set of data.

If the Ge(Li) detector is to operate in the anti-Compton mode or in coincidence with particles then an external reset is required for all nonvalid events, (e.g., Compton rejected events). The Ge(Li) signals and valid event gates are fed into the anti-coincidence reset circuit which provides the external reset. There is also an ADC busy input to prevent false resets while the computer is processing an event.

4. Analysis

In order to apply the formalism of section 2, one must provide the average γ-ray energy and then apply several corrections to the data.

4.1. Average γ-ray energy

Since there is some energy dependence of the NaI integral efficiency, $\bar{\Omega}$, of eq. (21), the average γ-ray

energy must be known for extracting multiplicities. Depending on the experiment there are several ways to arrive at $\bar{E}_\gamma$. If in simple reactions such as (α, p) one detects the outgoing proton, then kinematical considerations fix the excitation energy E^* in the product nucleus and hence implicitly define $\bar{E}_\gamma$ as equal to $E^*/\langle M\rangle$. A simple iterative procedure allows one to simultaneously solve for $\langle M\rangle$ and satisfy this constraint.

If one records as well the energy in the NaI detectors then knowledge of the response functions of the NaI detector enables one to unfold the NaI spectrum and thus determine the average γ-ray energy. For heavy-ion induced reactions it is possible to use an empirically derived formula due to Alexander and Natowitz[7]) in the same manner as ref. 4 to calculate the average available energy $\bar{E}^*$ for γ decay and thus solve for $\langle M_{in}\rangle$.

4.2. Angular correlation effects

The angular correlation corrections $\overline{W}_p$ in eq. (22) can be estimated by considering the simplest case of $\overline{W}_1$ for a highly aligned high-spin cascade of stretched E2 transitions using the formalism of Krane et al.[8]). One of the γ-rays is asssumed to be observed in the Ge(Li) detector and another in one of the NaI detectors. One then averages over all NaI detectors and obtains an average correction factor. The result is rather insensitive to the degree of assumed nuclear spin alignment. By careful choice of detector placement this correction can be kept small. For example in the geometry employed in ref. 4 $\overline{W}_1$ is 0.975. The corrections of $p \geq 2$ are expected to be somewhat larger due to possible increase in alignment when several members of the cascade are detected. In order to examine[4]) the effects of these corrections, the first three moments were compared under the following assumptions (a)

$$\overline{W}_1 = \overline{W}_2 = \ldots \overline{W}_{p\max}$$

and (b)

$$\overline{W}_p = \overline{W}_1 [1-(p-1)\tfrac{1}{2}(1-\overline{W}_1)].$$

We found that in case (b) $\langle M_{in}\rangle$, $\sigma_{M_{in}}$ and $s_{M_{in}}$ changed on the average by $+1.3\%$, $+1.6\%$ and -2.0% relative to the values obtained in case (a). Corrections for angular correlation effects are made according to the approximation (b) above.

4.3. Coincidence efficiency

In writing eq. (3) it was assumed that the experimental coincidence efficiency, ε, is unity. In this work the coincidence condition was established by overlap of the discriminator signals with a fixed resolving time given by the sum of the discriminator timing signals. In such a case due to poor timing characteristics of the Ge(Li) detector for a large dynamic range, one sometimes obtains a coincidence efficiency lower than unity, particularly at low energies. Corrections for this can be applied in the following manner:

$$C_0^{(\alpha)} = C_0^{(\alpha)'} P_{N0}^{(\alpha)} / P_{N0}^{(\alpha)'}, \tag{25}$$

with

$$P_{N0}^{(\alpha)} = (1-N\bar{\Omega}_{tot})^{M_{tot}-1} (1-N\Omega_{neut})^{x}, \tag{25a}$$

and

$$P_{N0}^{(\alpha)'} = (1-N\bar{\Omega}_{tot}\varepsilon)^{M_{tot}-1} (1-N\Omega_{neut}\varepsilon)^{x}, \tag{25b}$$

where $C_0^{(\alpha)'}$ are the uncorrected observed counts in the 0-fold (no coincidence) events; $\bar{\Omega}_{tot}$ and M_{tot} refer to total multiplicity, i.e., incoming as well as outgoing. Corrections for the p-fold coincidence counts are obtained as $C_P^{(\alpha)} = C_P^{(\alpha)'}[1-P_{N0}^{(\alpha)}]/[1-P_{N0}^{(\alpha)'}]$. The values to be used for $\bar{\Omega}_{tot}$ and M_{tot} are found by an iterative process. They are first obtained by using the uncorrected counts and by utilizing a zero order approximation to the general program. One solves iteratively eq. (25b) for Ω_{tot} and M_{tot}. Those values are then used to calculate the correction factor in eq. (25). The corrected counts are then used in the general program. The results of the complete calculation can then be used to recalculate the correction factor and the process is iterated. In general one or two complete iterations have been sufficient to obtain a self-consistent solution.

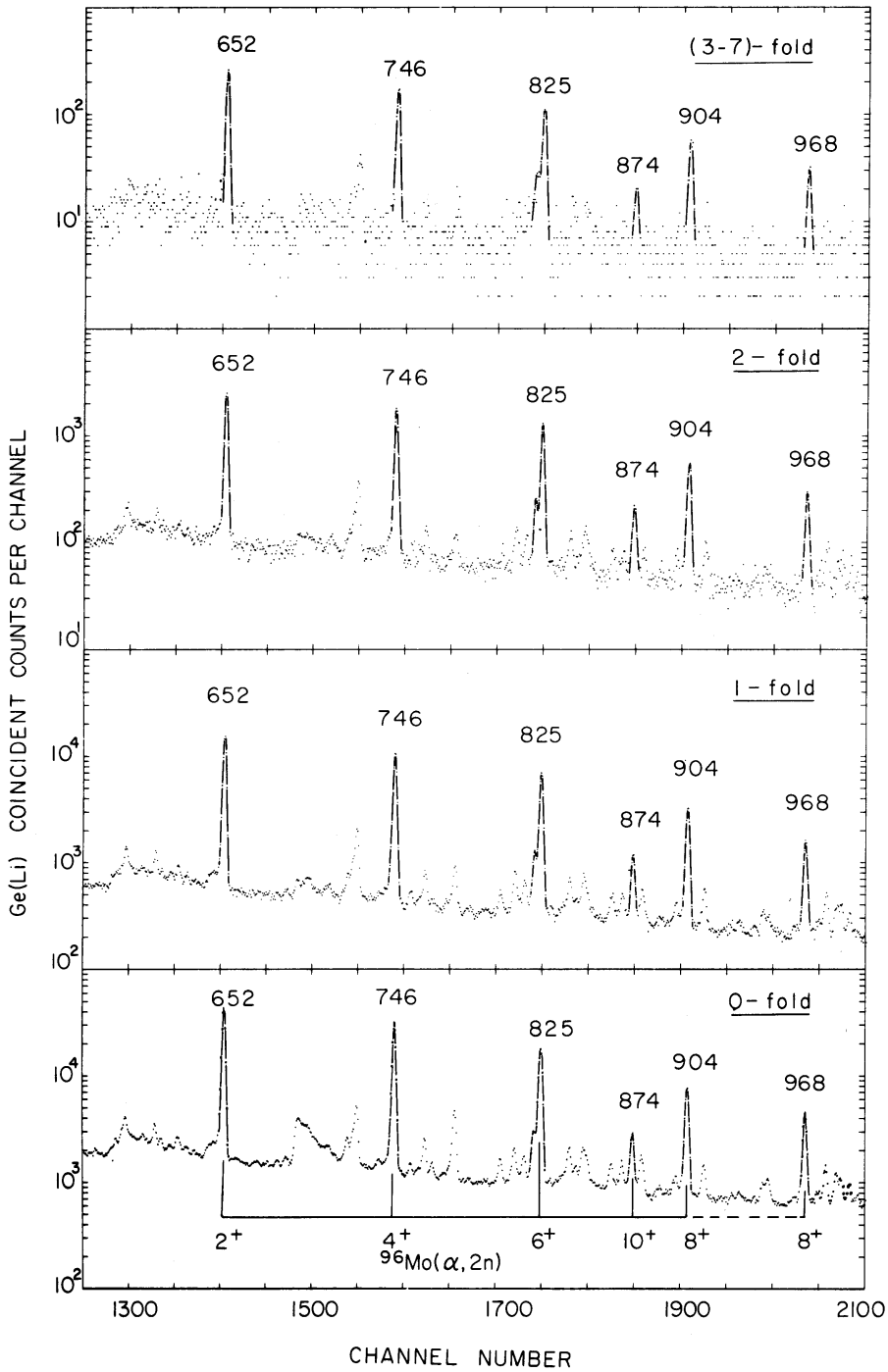

Fig. 7. Spectra recorded with a Ge(Li) γ-ray detector operated in the anti-Compton arrangement in multiple coincidence with 7 NaI detectors from a 30 MeV α-bombardment of ^{96}Mo. The 0-fold refers to no coincidence and the (3–7)-fold to the sum of 3- through 7-fold coincidences. Only the prominant γ-rays from the (α, 2n) reaction are labelled.

The coincidence efficiency, ε, is computed from analysis of multiplicity as a function of energy over the Compton distribution from a source with known simple multiplicity, e.g. ^{60}Co.

4.4. Corrections for random coincidences

In order to estimate the correction due to random coincidences a pulser triggered by the digital output of the current integrator is connected to the Ge(Li) preamplifier. One then obtains the random correction by a comparison of the counts due to the pulser in the 0-fold, $C_0^{(p)}$, to the pulser counts in the higher folds, $C_k^{(p)}$. The correction is applied to the experimentally derived probabilities according to

$$P_{N0}^{(\alpha)} = P_{N0}^{(\alpha)'} + 1 - f_0^{(p)}, \tag{26}$$

and

$$P_{Nk}^{(\alpha)} = P_{Nk}^{(\alpha)'} - f_k^{(p)}, \tag{27}$$

Table 1

Input data for program GETM.

Required data	See section
γ-calibrations	
Calibration energy points	
NaI integral efficiencies	
M1 and E2 conversion coefficients	
Coincidence efficiencies	4.3
Ge(Li) integral efficiencies	4.5
Ge(Li) absolute photo-peak efficiencies	
Pulser counts for randoms correction	4.4
Level scheme	
Number of levels in scheme	
Level energies	
Branching ratios for all levels	
Fraction of each discrete state transition that is M1	
Cross section	4.5
Target mass	
Effective charge of projectile	
Target thickness	
Isotopic abundance	5
Integrator counts and calibration constant	
Angular distribution correction factor	
Angular correlation correction for summing in Ge(Li)	
Multiplicity	
Highest fold utilized in the calculation	
Number of NaI detectors	
Neutron multiplicity	5
Average neutron efficiency in the NaI	5
Energy available for γ-decay, or average energy per γ-ray	4.1
Angular correlation correction for Ge(Li) – NaI coincidences	4.2
Fraction of continuum decay that is M1	
Side feeding fractions	
Discrete-state feeding fractions	
Coincidence counts for each fold and their errors	

where

$$f_k^{(p)} = \frac{C_k^{(p)}}{\sum_{i=0}^{N_{max}} C_i^{(p)}}. \tag{27a}$$

$P_{N0}^{(\alpha)'}$ and $P_{Nk}^{(\alpha)'}$ are the uncorrected 0-fold and k-fold probabilities, respectively.

4.5. Example of analysis

A computer code called GETM was written in Fortran IV to perform the algebra indicated in section 2. In particular, it employs the R-method for the calculation of multiplicities and higher moments. In addition, the code utilizes the already available information on γ-ray yields and detector efficiencies to calculate cross sections for the population of the various levels. The code also includes the corrections discussed in sections 4.1–4.4.

The input for GETM consists of four basic types of data; (a) calibrations, (b) levels scheme, (c) cross section and (d) multiplicity. The data required are indicated in table 1. Side-feeding fractions can be read in, if known, for each level.

The spectra of fig. 7 are from a 4.3 h run with the anti-Compton geometry at the Washington University cyclotron. ^{96}Mo was bombarded with 30 MeV alpha particles. Spectra corresponding to 0-, 1-, 2- and 3-fold coincidences were recorded. Coincidences of higher order were added to the 3-fold events. The peak areas of the 652 keV $2^+ \rightarrow 0^+$ transition in ^{98}Ru were determined for all folds and were used as input to the multiplicity code GETM. A copy of the output from the program is shown in fig. 8. In the code the ground state is numbered 1. The columns labelled PN and EPN are the experimental P_{Np} values of eq. (3) and their errors without any corrections. In the next line the interpolated coincidence efficiency, ε, and M_{tot} of eq. (25b) are given together with the approximate average energy used

```
 96MO(ALPHA,2N)98RU  E(ALPHA)= 30 MEV
 INITIAL LEVEL NO.=  2, FINAL LEVEL NO.=  1, LEVEL ENERGY=   652.41, TRANSITION ENERGY=   652.41

 INPUT DATA
FOLD     COUNTS       ERROR
 0      167407.0      1881.0
 1       62603.0       832.0
 2       10066.0       384.0
 3        1004.0        39.0
SUM     241080.0      2092.7
FOLD        PN           EPN
 0      0.6944043    0.0082375
 1      0.2596772    0.0040235
 2      0.0417538    0.0016322
 3      0.0041646    0.0001658
COINC. EFF.=  1.0000, CALCULATED MTOTAL=    7.260 AND AVER. EN. =  1469.7
FOLD     L(P,0)       L(P,1)       L(P,2)       L(P,3)
 1   -0.99760151   0.99760151  -0.49880075   0.16626692
 2   -0.99999726   0.00479221   0.99280977  -0.99440718
 3   -1.00000000   0.00000858   0.00717354   0.98563635

 CORRECTED DATA
FOLD   COUNTS     SIG C       PN        SIG PN         R          SIG R          X          SIGX
 0    168554.    1944.    0.699162   0.008063
 1     60932.    1005.    0.252747   0.004171     0.0503086   0.0007982   0.0495181   0.00079953
 2     10477.     442.    0.043460   0.001835     0.0027311   0.0000919   0.0026238   0.00009169
 3      1116.      46.    0.004631   0.000198     0.0001323   0.0000057   0.0001146   0.00000574

SIDE FEEDING FRACTION=1,  RESULTS OBTAINED WITH COMPLETE DECAY SCHEME BELOW
M(IN)=    6.341 +-    0.103    M(OUT)=      1.000   M(TOTAL)=    7.341
SIGMA=    3.054 +-    0.327    E(AVG)=   1347.98
SKEW =   -1.905 +-    1.164    OMEG(AVG)=   0.007794

CROSS SECTION =  1072.46 +/-    9.31 MILLIBARNS
```

Fig. 8. Sample output of the computer code GETM for the 652 keV $2^+ \rightarrow 0^+$ transition of ^{98}Ru.

to compute M_{tot}. The quantities labelled L(P,I) are the $\lambda_{p,r}$ matrix elements of eq. (20a). The $\lambda_{p,0}$ values differ slightly from unity and the elements below the diagonal differ from zero because of the exact treatment for the transitions below the gating transition and because of the correction for neutron response of the NaI detectors [$(K_k^{(j)}$ and $K_k^{(neut)}$ terms in eq. (20a)]. Under the heading "corrected data" the counts, the P_{Np}, R_p and X_r values from eqs. (3), (18) and (17b) and their errors are given corrected for angular correlation effects, coincidence efficiency and random coincidences. The values for M_{in}, M_{out} and $M_{tot} = M_{in} + M_{out}$ are given together with the width $\sigma_{M_{in}}$ (labelled SIGMA), the skewness $s_{M_{in}}$ (labelled SKEW), the average γ-ray energy for the incoming cascade [labelled E(AVG)] and the average NaI efficiency for the incoming cascade [labelled OMEG(AVG)]. Finally, the cross section was computed with the formula:

$$\sigma = \frac{0.0022803\, dAZ_{eff}\, C_\gamma (1+\alpha_T)}{abtQ\Omega_{Ge}\,(1-\Omega_0 W_1)^{M_{tot}-1}\, W(90)}\ [\mathrm{mb}]\,. \tag{28}$$

d is the current-integrator calibration constant, A is the target mass [amu], Z_{eff} is the effective charge, C_γ is the sum of all folds, α_T is the total conversion coefficient, a is the fractional isotopic abundance, b is the branching ratio, t is the target thickness [mg/cm^2], Q is the collected charge [10^{-10} C], Ω_{Ge} is the absolute photo-peak efficiency, Ω_0 is the integral Ge(Li) efficiency, W_1 is the angular correlation correction for detecting any two of the γ-rays in the cascade in the Ge(Li) detector, M_{tot} is total multiplicity in the cascade, and $W(90)$ is the angular distribution of the gating transition. The term $(1-\Omega_0 W_1)^{M_{tot}-1}$ in the denominator of eq. (28) corrects for losses due to coincidence summing in the Ge(Li) detector itself. The integral efficiency Ω_0 in eq. (28) should include all true counts recorded down to zero energy, taken, for example, with an analyzer in singles live-time mode.

5. Concluding remarks

The integral efficiency for one NaI detector in the apparatus is typically 0.0106, 0.0100, 0.0090, 0.0084, 0.0081 and 0.0080 at 200, 400, 600, 1000, 1250 and 2754 keV, respectively. The flattening of the efficiency curve at high energies is due to the increasing pair production and scattering from the lead shield into the detectors.

The efficiency of the NaI detectors for neutrons was measured by recording the time-of-flight to a NaI detector placed at 1 m. A coincidence requirement with one NaI detector placed close to the target helps in reducing the background in the time-of-flight spectrum. A beam of 14 MeV α-particles was used in the ^{95}Mo(α, nγ)^{98}Ru reaction[4]). The neutron efficiency of the NaI was found to be (14±4)% of the γ-ray efficiency for an average γ-ray energy of 700 keV.

The apparatus described here has been found very flexible in allowing several types of experiments to be performed with only minor changes in configuration. The anti-Compton geometry permits measurement of multiplicity for low-cross-section reaction channels.

It is interesting to note that for heavy-ion induced reactions with high multiplicities (20–30) the 0-fold spectrum contains only a small fraction of the total peak intensity. It also has all the background events.

Finally, it should be noted that the use of targets of highest possible chemical abundance is important, since impurities of neighboring isotopes may give rise to the same final nucleus via a different reaction and thus result in an erroneous multiplicity.

We are very grateful to the staff of the Washington University cyclotron and the machine shop for their excellent work in construction of the apparatus. One of us, J. H. Barker, would like to thank the Research Corporation for support during this work.

Appendix

Let $S_{np} = \sum_{n_1 \ldots n_N} \delta^{N-p}_{\delta^0_{n_1} + \ldots + \delta^0_{n_N}}\, \delta^n_{n_1 + \ldots + n_N} \dfrac{1}{\prod_j \prod_j n!}$.

Then $\sum_{n,p=0}^{\infty} S_{np} u^n v^p = \sum_{n_1 \ldots n_N} \frac{1}{\prod_j n_j!} u^{n_1 + \ldots + n_N} v^{N - \delta^0_{n_1} - \ldots - \delta^0_{n_N}} = v^N \sum_{n_1 \ldots n_N} \prod_j \left(\frac{u^{n_j}}{n_j!\, v^{\delta^0_{n_j}}} \right)$

$$= v^N \prod_j \sum_{n_j} \frac{u^{n_j}}{v^{\delta^0_{n_j}} n_j!} = v^N \left(\frac{1}{v} + e^u - 1 \right)^N = [1 + v(e^u - 1)]^N .$$

It only remains to re-expand in u and v to determine the S_{np} as follows:

$$\sum_{n,p=0}^{\infty} S_{np} u^n v^p = \sum_{p=0}^{\infty} \binom{N}{p} v^p (e^u - 1)^p = \sum_{p=0}^{\infty} v^p \binom{N}{p} \sum_{k=0}^{p} \binom{p}{k} e^{ku} (-1)^{p-k}$$

$$= \sum_{n,p=0}^{\infty} v^p u^n \frac{1}{n!} \binom{N}{p} \sum_{k=0}^{p} \binom{p}{k} (-1)^{p-k} k^n .$$

Therefore, $S_{np} = \frac{1}{n!} \binom{N}{p} (-1)^p \sum_{k=0}^{p} \binom{p}{k} (-1)^k k^n .$

References

[1] P. O. Tjøm, F. S. Stephens, R. M. Diamond, J. de Boer and W. M. Meyerhof, Phys. Rev. Lett. **33** (1974) 593.
[2] E. der Mateosian, O. C. Kistner and A. W. Sunyar, Phys. Rev. Lett. **33** (1974) 596.
[3] G. B. Hagemann, R. Broda, B. Herskind, M. Ishihara, S. Ogaza and H. Ryde, Nucl. Phys. **A245** (1975) 166.
[4] D. G. Sarantites, J. H. Barker, M. L. Halbert, D. C. Hensley, R. A. Dayras, E. Eichler, N. R. Johnson and S. A. Gronemeyer, Phys. Rev. **C14** (1976) 2138.
[5] D. G. Sarantites, L. Westerberg, J. H. Barker, M. L. Halbert, R.A. Dayras and D. C. Hensley, to be published.
[6] R. A. Dayras, R. G. Stokstad, D. C. Hensley, M. L. Halbert, C. B. Fulmer, A. H. Snell, R. L. Robinson, D. G. Sarantites and L. Westerberg, to be published.
[7] J. M. Alexander and J. B. Natowitz, Phys. Rev. **188** (1969) 1842.
[8] K. S. Krane, R. M. Steffen and R. M. Wheeler, Nucl. Data Tables **11** (1973) 351.